Photon Events with Missing Energy at $\sqrt{s}$ =183 to 189 GeV

DELPHI Collaboration

Abstract

The production of single photons has been studied in the reaction $e^+e^- \to \gamma + invisible\ particles$ at centre-of-mass energies of 183 GeV and 189 GeV. A previously published analysis of events with multi-photon final states accompanied by missing energy has been updated with 189 GeV data. The data were collected with the DELPHI detector and correspond to integrated luminosities of about 51 pb^{-1} and 158 pb^{-1} at the two energies. The number of light neutrino families is measured to be $2.84 \pm 0.15(stat) \pm 0.14(syst)$. The absence of an excess of events beyond that expected from Standard Model processes is used to set limits on new physics as described by supersymmetric and composite models. A limit on the gravitational scale is also determined.

P.Abreu[22], W.Adam[52], T.Adye[38], P.Adzic[12], I.Ajinenko[44], Z.Albrecht[18], T.Alderweireld[2], G.D.Alekseev[17], R.Alemany[51], T.Allmendinger[18], P.P.Allport[23], S.Almehed[25], U.Amaldi[29], N.Amapane[47], S.Amato[49], E.G.Anassontzis[3], P.Andersson[46], A.Andreazza[9], S.Andringa[22], P.Antilogus[26], W-D.Apel[18], Y.Arnoud[9], B.Åsman[46], J-E.Augustin[26], A.Augustinus[9], P.Baillon[9], P.Bambade[20], F.Barao[22], G.Barbiellini[48], R.Barbier[26], D.Y.Bardin[17], G.Barker[18], A.Baroncelli[40], M.Battaglia[16], M.Baubillier[24], K-H.Becks[54], M.Begalli[6], A.Behrmann[54], P.Beilliere[8], Yu.Belokopytov[9], N.C.Benekos[33], A.C.Benvenuti[5], C.Berat[15], M.Berggren[24], D.Bertrand[2], M.Besancon[41], M.Bigi[47], M.S.Bilenky[17], M-A.Bizouard[20], D.Bloch[10], H.M.Blom[32], M.Bonesini[29], M.Boonekamp[41], P.S.L.Booth[23], A.W.Borgland[4], G.Borisov[20], C.Bosio[43], O.Botner[50], E.Boudinov[32], B.Bouquet[20], C.Bourdarios[20], T.J.V.Bowcock[23], I.Boyko[17], I.Bozovic[12], M.Bozzo[14], M.Bracko[45], P.Branchini[40], R.A.Brenner[50], P.Bruckman[9], J-M.Brunet[8], L.Bugge[34], T.Buran[34], B.Buschbeck[52], P.Buschmann[54], S.Cabrera[51], M.Caccia[28], M.Calvi[29], T.Camporesi[9], V.Canale[39], F.Carena[9], L.Carroll[23], C.Caso[14], M.V.Castillo Gimenez[51], A.Cattai[9], F.R.Cavallo[5], V.Chabaud[9], Ph.Charpentier[9], P.Checchia[37], G.A.Chelkov[17], R.Chierici[47], P.Chliapnikov[9,44], P.Chochula[7], V.Chorowicz[26], J.Chudoba[31], K.Cieslik[19], P.Collins[9], R.Contri[14], E.Cortina[51], G.Cosme[20], F.Cossutti[9], H.B.Crawley[1], D.Crennell[38], S.Crepe[15], G.Crosetti[14], J.Cuevas Maestro[35], S.Czellar[16], M.Davenport[9], W.Da Silva[24], G.Della Ricca[48], P.Delpierre[27], N.Demaria[9], A.De Angelis[48], W.De Boer[18], C.De Clercq[2], B.De Lotto[48], A.De Min[37], L.De Paula[49], H.Dijkstra[9], L.Di Ciaccio[9,39], J.Dolbeau[8], K.Doroba[53], M.Dracos[10], J.Drees[54], M.Dris[33], A.Duperrin[26], J-D.Durand[9], G.Eigen[4], T.Ekelof[50], G.Ekspong[46], M.Ellert[50], M.Elsing[9], J-P.Engel[10], M.Espirito Santo[22], E.Falk[25], G.Fanourakis[12], D.Fassouliotis[12], J.Fayot[24], M.Feindt[18], P.Ferrari[28], A.Ferrer[51], E.Ferrer-Ribas[20], F.Ferro[14], S.Fichet[24], A.Firestone[1], U.Flagmeyer[54], H.Foeth[9], E.Fokitis[33], F.Fontanelli[14], B.Franek[38], A.G.Frodesen[4], R.Fruhwirth[52], F.Fulda-Quenzer[20], J.Fuster[51], A.Galloni[23], D.Gamba[47], S.Gamblin[20], M.Gandelman[49], C.Garcia[51], C.Gaspar[9], M.Gaspar[49], U.Gasparini[37], Ph.Gavillet[9], E.N.Gazis[33], D.Gele[10], L.Gerdyukov[44], N.Ghodbane[26], I.Gil[51], F.Glege[54], R.Gokieli[9,53], B.Golob[9,45], G.Gomez-Ceballos[42], P.Goncalves[22], I.Gonzalez Caballero[42], G.Gopal[38], L.Gorn[1], Yu.Gouz[44], V.Gracco[14], J.Grahl[1], E.Graziani[40], P.Gris[41], G.Grosdidier[20], K.Grzelak[53], J.Guy[38], C.Haag[18], F.Hahn[9], S.Hahn[54], S.Haider[9], A.Hallgren[50], K.Hamacher[54], J.Hansen[34], F.J.Harris[36], V.Hedberg[9,25], S.Heising[18], J.J.Hernandez[51], P.Herquet[2], H.Herr[9], T.L.Hessing[36], J.-M.Heuser[54], E.Higon[51], S-O.Holmgren[46], P.J.Holt[36], S.Hoorelbeke[2], M.Houlden[23], J.Hrubec[52], M.Huber[18], K.Huet[2], G.J.Hughes[23], K.Hultqvist[9,46], J.N.Jackson[23], R.Jacobsson[9], P.Jalocha[19], R.Janik[7], Ch.Jarlskog[25], G.Jarlskog[25], P.Jarry[41], B.Jean-Marie[20], D.Jeans[36], E.K.Johansson[46], P.Jonsson[26], C.Joram[9], P.Juillot[10], L.Jungermann[18], F.Kapusta[24], K.Karafasoulis[12], S.Katsanevas[26], E.C.Katsoufis[33], R.Keranen[18], G.Kernel[45], B.P.Kersevan[45], Yu.Khokhlov[44], B.A.Khomenko[17], N.N.Khovanski[17], A.Kiiskinen[16], B.King[23], A.Kinvig[23], N.J.Kjaer[9], O.Klapp[54], H.Klein[9], P.Kluit[32], P.Kokkinias[12], V.Kostioukhine[44], C.Kourkoumelis[3], O.Kouznetsov[41], M.Krammer[52], E.Kriznic[45], Z.Krumstein[17], P.Kubinec[7], J.Kurowska[53], K.Kurvinen[16], J.W.Lamsa[1], D.W.Lane[1], V.Lapin[44], J-P.Laugier[41], R.Lauhakangas[16], G.Leder[52], F.Ledroit[15], V.Lefebure[2], L.Leinonen[46], A.Leisos[12], R.Leitner[31], J.Lemonne[2], G.Lenzen[54], V.Lepeltier[20], T.Lesiak[19], M.Lethuillier[41], J.Libby[36], W.Liebig[54], D.Liko[9], A.Lipniacka[9,46], I.Lippi[37], B.Loerstad[25], J.G.Loken[36], J.H.Lopes[49], J.M.Lopez[42], R.Lopez-Fernandez[15], D.Loukas[12], P.Lutz[41], L.Lyons[36], J.MacNaughton[52], J.R.Mahon[6], A.Maio[22], A.Malek[54], T.G.M.Malmgren[46], S.Maltezos[33], V.Malychev[17], F.Mandl[52], J.Marco[42], R.Marco[42], B.Marechal[49], M.Margoni[37], J-C.Marin[9], C.Mariotti[9], A.Markou[12], C.Martinez-Rivero[20], F.Martinez-Vidal[51], S.Marti i Garcia[9], J.Masik[13], N.Mastroyiannopoulos[12], F.Matorras[42], C.Matteuzzi[29], G.Matthiae[39], F.Mazzucato[37], M.Mazzucato[37], M.Mc Cubbin[23], R.Mc Kay[1], R.Mc Nulty[23], G.Mc Pherson[23], C.Meroni[28], W.T.Meyer[1], E.Migliore[9], L.Mirabito[26], W.A.Mitaroff[52], U.Mjoernmark[25], T.Moa[46], M.Moch[18], R.Moeller[30], K.Moenig[9,11], M.R.Monge[14], D.Moraes[49], X.Moreau[24], P.Morettini[14], G.Morton[36], U.Mueller[54], K.Muenich[54], M.Mulders[32], C.Mulet-Marquis[15], R.Muresan[25], W.J.Murray[38], B.Muryn[19], G.Myatt[36], T.Myklebust[34], F.Naraghi[15], M.Nassiakou[12], F.L.Navarria[5], S.Navas[51], K.Nawrocki[53], P.Negri[29], N.Neufeld[9], R.Nicolaidou[41], B.S.Nielsen[30], P.Niezurawski[53], M.Nikolenko[10,17], V.Nomokonov[16], A.Nygren[25], V.Obraztsov[44], A.G.Olshevski[17], A.Onofre[22], R.Orava[16], G.Orazi[10], K.Osterberg[16], A.Ouraou[41], M.Paganoni[29], S.Paiano[5], R.Pain[24], R.Paiva[22], J.Palacios[36], H.Palka[19], Th.D.Papadopoulou[9,33], K.Papageorgiou[12], L.Pape[9], C.Parkes[9], F.Parodi[14], U.Parzefall[23], A.Passeri[40], O.Passon[54], T.Pavel[25], M.Pegoraro[37], L.Peralta[22], M.Pernicka[52], A.Perrotta[5], C.Petridou[48], A.Petrolini[14], H.T.Phillips[38], F.Pierre[41], M.Pimenta[22], E.Piotto[28], T.Podobnik[45], M.E.Pol[6], G.Polok[19], P.Poropat[48], V.Pozdniakov[17], P.Privitera[39], N.Pukhaeva[17], A.Pullia[29], D.Radojicic[36], S.Ragazzi[29], H.Rahmani[33], J.Rames[13], P.N.Ratoff[21], A.L.Read[34], P.Rebecchi[9], N.G.Redaelli[29], M.Regler[52], J.Rehn[18], D.Reid[32], R.Reinhardt[54], P.B.Renton[36], L.K.Resvanis[3], F.Richard[20], J.Ridky[13], G.Rinaudo[47], I.Ripp-Baudot[10], O.Rohne[34], A.Romero[47], P.Ronchese[37], E.I.Rosenberg[1], P.Rosinsky[7], P.Roudeau[20], T.Rovelli[5], Ch.Royon[41], V.Ruhlmann-Kleider[41], A.Ruiz[42], H.Saarikko[16], Y.Sacquin[41], A.Sadovsky[17], G.Sajot[15], J.Salt[51], D.Sampsonidis[12], M.Sannino[14], Ph.Schwemling[24], B.Schwering[54], U.Schwickerath[18], F.Scuri[48], P.Seager[21], Y.Sedykh[17], A.M.Segar[36], N.Seibert[18], R.Sekulin[38], R.C.Shellard[6], M.Siebel[54], L.Simard[41], F.Simonetto[37], A.N.Sisakian[17], G.Smadja[26], N.Smirnov[44], O.Smirnova[25], G.R.Smith[38], A.Sokolov[44], A.Sopczak[18], R.Sosnowski[53], T.Spassov[22], E.Spiriti[40], S.Squarcia[14], C.Stanescu[40], S.Stanic[45], M.Stanitzki[18], K.Stevenson[36], A.Stocchi[20], J.Strauss[52], R.Strub[10], B.Stugu[4], M.Szczekowski[53], M.Szeptycka[53], T.Tabarelli[29], A.Taffard[23], F.Tegenfeldt[50], F.Terranova[29], J.Thomas[36], J.Timmermans[32], N.Tinti[5], L.G.Tkatchev[17], M.Tobin[23], S.Todorova[10], A.Tomaradze[2], B.Tome[22], A.Tonazzo[9], L.Tortora[40], P.Tortosa[51], G.Transtromer[25], D.Treille[9],

G.Tristram[8], M.Trochimczuk[53], C.Troncon[28], M-L.Turluer[41], I.A.Tyapkin[17], S.Tzamarias[12], O.Ullaland[9], V.Uvarov[44], G.Valenti[9,5], E.Vallazza[48], P.Van Dam[32], W.Van den Boeck[2], J.Van Eldik[9,32], A.Van Lysebetten[2], N.van Remortel[2], I.Van Vulpen[32], G.Vegni[28], L.Ventura[37], W.Venus[38,9], F.Verbeure[2], P.Verdier[26], M.Verlato[37], L.S.Vertogradov[17], V.Verzi[28], D.Vilanova[41], L.Vitale[48], E.Vlasov[44], A.S.Vodopyanov[17], G.Voulgaris[3], V.Vrba[13], H.Wahlen[54], C.Walck[46], A.J.Washbrook[23], C.Weiser[9], D.Wicke[54], J.H.Wickens[2], G.R.Wilkinson[36], M.Winter[10], M.Witek[19], G.Wolf[9], J.Yi[1], O.Yushchenko[44], A.Zalewska[19], P.Zalewski[53], D.Zavrtanik[45], E.Zevgolatakos[12], N.I.Zimin[17,25], A.Zintchenko[17], Ph.Zoller[10], G.C.Zucchelli[46], G.Zumerle[37]

[1]Department of Physics and Astronomy, Iowa State University, Ames IA 50011-3160, USA
[2]Physics Department, Univ. Instelling Antwerpen, Universiteitsplein 1, B-2610 Antwerpen, Belgium
   and IIHE, ULB-VUB, Pleinlaan 2, B-1050 Brussels, Belgium
   and Faculté des Sciences, Univ. de l'Etat Mons, Av. Maistriau 19, B-7000 Mons, Belgium
[3]Physics Laboratory, University of Athens, Solonos Str. 104, GR-10680 Athens, Greece
[4]Department of Physics, University of Bergen, Allégaten 55, NO-5007 Bergen, Norway
[5]Dipartimento di Fisica, Università di Bologna and INFN, Via Irnerio 46, IT-40126 Bologna, Italy
[6]Centro Brasileiro de Pesquisas Físicas, rua Xavier Sigaud 150, BR-22290 Rio de Janeiro, Brazil
   and Depto. de Física, Pont. Univ. Católica, C.P. 38071 BR-22453 Rio de Janeiro, Brazil
   and Inst. de Física, Univ. Estadual do Rio de Janeiro, rua São Francisco Xavier 524, Rio de Janeiro, Brazil
[7]Comenius University, Faculty of Mathematics and Physics, Mlynska Dolina, SK-84215 Bratislava, Slovakia
[8]Collège de France, Lab. de Physique Corpusculaire, IN2P3-CNRS, FR-75231 Paris Cedex 05, France
[9]CERN, CH-1211 Geneva 23, Switzerland
[10]Institut de Recherches Subatomiques, IN2P3 - CNRS/ULP - BP20, FR-67037 Strasbourg Cedex, France
[11]Now at DESY-Zeuthen, Platanenallee 6, D-15735 Zeuthen, Germany
[12]Institute of Nuclear Physics, N.C.S.R. Demokritos, P.O. Box 60228, GR-15310 Athens, Greece
[13]FZU, Inst. of Phys. of the C.A.S. High Energy Physics Division, Na Slovance 2, CZ-180 40, Praha 8, Czech Republic
[14]Dipartimento di Fisica, Università di Genova and INFN, Via Dodecaneso 33, IT-16146 Genova, Italy
[15]Institut des Sciences Nucléaires, IN2P3-CNRS, Université de Grenoble 1, FR-38026 Grenoble Cedex, France
[16]Helsinki Institute of Physics, HIP, P.O. Box 9, FI-00014 Helsinki, Finland
[17]Joint Institute for Nuclear Research, Dubna, Head Post Office, P.O. Box 79, RU-101 000 Moscow, Russian Federation
[18]Institut für Experimentelle Kernphysik, Universität Karlsruhe, Postfach 6980, DE-76128 Karlsruhe, Germany
[19]Institute of Nuclear Physics and University of Mining and Metalurgy, Ul. Kawiory 26a, PL-30055 Krakow, Poland
[20]Université de Paris-Sud, Lab. de l'Accélérateur Linéaire, IN2P3-CNRS, Bât. 200, FR-91405 Orsay Cedex, France
[21]School of Physics and Chemistry, University of Lancaster, Lancaster LA1 4YB, UK
[22]LIP, IST, FCUL - Av. Elias Garcia, 14-1º, PT-1000 Lisboa Codex, Portugal
[23]Department of Physics, University of Liverpool, P.O. Box 147, Liverpool L69 3BX, UK
[24]LPNHE, IN2P3-CNRS, Univ. Paris VI et VII, Tour 33 (RdC), 4 place Jussieu, FR-75252 Paris Cedex 05, France
[25]Department of Physics, University of Lund, Sölvegatan 14, SE-223 63 Lund, Sweden
[26]Université Claude Bernard de Lyon, IPNL, IN2P3-CNRS, FR-69622 Villeurbanne Cedex, France
[27]Univ. d'Aix - Marseille II - CPP, IN2P3-CNRS, FR-13288 Marseille Cedex 09, France
[28]Dipartimento di Fisica, Università di Milano and INFN-MILANO, Via Celoria 16, IT-20133 Milan, Italy
[29]Dipartimento di Fisica, Univ. di Milano-Bicocca and INFN-MILANO, Piazza delle Scienze 2, IT-20126 Milan, Italy
[30]Niels Bohr Institute, Blegdamsvej 17, DK-2100 Copenhagen Ø, Denmark
[31]IPNP of MFF, Charles Univ., Areal MFF, V Holesovickach 2, CZ-180 00, Praha 8, Czech Republic
[32]NIKHEF, Postbus 41882, NL-1009 DB Amsterdam, The Netherlands
[33]National Technical University, Physics Department, Zografou Campus, GR-15773 Athens, Greece
[34]Physics Department, University of Oslo, Blindern, NO-1000 Oslo 3, Norway
[35]Dpto. Fisica, Univ. Oviedo, Avda. Calvo Sotelo s/n, ES-33007 Oviedo, Spain
[36]Department of Physics, University of Oxford, Keble Road, Oxford OX1 3RH, UK
[37]Dipartimento di Fisica, Università di Padova and INFN, Via Marzolo 8, IT-35131 Padua, Italy
[38]Rutherford Appleton Laboratory, Chilton, Didcot OX11 OQX, UK
[39]Dipartimento di Fisica, Università di Roma II and INFN, Tor Vergata, IT-00173 Rome, Italy
[40]Dipartimento di Fisica, Università di Roma III and INFN, Via della Vasca Navale 84, IT-00146 Rome, Italy
[41]DAPNIA/Service de Physique des Particules, CEA-Saclay, FR-91191 Gif-sur-Yvette Cedex, France
[42]Instituto de Fisica de Cantabria (CSIC-UC), Avda. los Castros s/n, ES-39006 Santander, Spain
[43]Dipartimento di Fisica, Università degli Studi di Roma La Sapienza, Piazzale Aldo Moro 2, IT-00185 Rome, Italy
[44]Inst. for High Energy Physics, Serpukov P.O. Box 35, Protvino, (Moscow Region), Russian Federation
[45]J. Stefan Institute, Jamova 39, SI-1000 Ljubljana, Slovenia and Laboratory for Astroparticle Physics,
   Nova Gorica Polytechnic, Kostanjeviska 16a, SI-5000 Nova Gorica, Slovenia,
   and Department of Physics, University of Ljubljana, SI-1000 Ljubljana, Slovenia
[46]Fysikum, Stockholm University, Box 6730, SE-113 85 Stockholm, Sweden
[47]Dipartimento di Fisica Sperimentale, Università di Torino and INFN, Via P. Giuria 1, IT-10125 Turin, Italy
[48]Dipartimento di Fisica, Università di Trieste and INFN, Via A. Valerio 2, IT-34127 Trieste, Italy
   and Istituto di Fisica, Università di Udine, IT-33100 Udine, Italy
[49]Univ. Federal do Rio de Janeiro, C.P. 68528 Cidade Univ., Ilha do Fundão BR-21945-970 Rio de Janeiro, Brazil
[50]Department of Radiation Sciences, University of Uppsala, P.O. Box 535, SE-751 21 Uppsala, Sweden
[51]IFIC, Valencia-CSIC, and D.F.A.M.N., U. de Valencia, Avda. Dr. Moliner 50, ES-46100 Burjassot (Valencia), Spain
[52]Institut für Hochenergiephysik, Österr. Akad. d. Wissensch., Nikolsdorfergasse 18, AT-1050 Vienna, Austria
[53]Inst. Nuclear Studies and University of Warsaw, Ul. Hoza 69, PL-00681 Warsaw, Poland
[54]Fachbereich Physik, University of Wuppertal, Postfach 100 127, DE-42097 Wuppertal, Germany

1   Introduction

At LEP2, the Standard Model predicts that events with one or more photons and invisible particles are produced exclusively by the reaction $e^+e^- \rightarrow \nu\bar{\nu}\gamma(\gamma)$ which receives a contribution from Z-exchange in the s-channel with single- or multi-photon emission from the initial state electrons and from the t-channel W exchange, with the photon(s) radiated from the beam electrons or the exchanged W.

Beyond the Standard Model, contributions to the γ + *missing energy* final state could come from a new generation of neutrinos, from the radiative production of some new particle, stable or unstable, weakly interacting or decaying into a photon. Theories of supersymmetry (SUSY) predict the existence of particles, such as the neutralino, which would produce a final state with missing energy and a photon if the lightest neutralino decays into $\tilde{G}\gamma$ with an essentially massless gravitino [1,2] and several results have been published on the search for $e^+e^- \rightarrow \tilde{G}\tilde{\chi}_1^0 \rightarrow \tilde{G}\tilde{G}\gamma$ [3,4,5]. If the gravitino is the only supersymmetric particle light enough to be produced, the expected cross-section for $e^+e^- \rightarrow \tilde{G}\tilde{G}\gamma$ can instead be used to set a lower limit on the gravitino mass [6].

Also in the same SUSY theoretical framework, multi-photon final states with missing energy could be a signature for neutralino pair-production, i.e. reactions of type $e^+e^- \rightarrow \tilde{\chi}_1^0\tilde{\chi}_1^0 \rightarrow \tilde{G}\gamma\tilde{G}\gamma$ [1,2] and $e^+e^- \rightarrow \tilde{\chi}_2^0\tilde{\chi}_2^0 \rightarrow \tilde{\chi}_1^0\gamma\tilde{\chi}_1^0\gamma$ [7]. In the case of long neutralino lifetimes the photons would not originate at the beam interaction region and could have a large impact parameter. For mean decay paths comparable to the detector scale, events with a single photon not pointing to the interaction region are expected.

In the study presented here, the single- and the multi-photon final states at LEP2 are used to explore the existence of possible new particles. After a brief description of the detectors used in the analysis and the selection criteria, a measurement of the number of neutrino families is made and limits on non-Standard Model physics, such as high-dimensional gravitons [8,9], compositeness [10] and supersymmetric particles, are presented.

This paper describes the analysis of single photon events collected by DELPHI at centre-of-mass energies ($\sqrt{s}$) of 183 GeV and 189 GeV at LEP during 1997 and 1998. The integrated luminosities at these energies were 51 pb^{-1} and 158 pb^{-1} respectively. Single non-pointing photons and multi-photon events have also been studied, but in this case the analysis is restricted to the data taken at $\sqrt{s} = 189$ GeV, since the results obtained at lower energies have already been published elsewhere [11]. The limits set on new phenomena take into account the lower energy data.

2   The DELPHI detector

The general criteria for the selection of events are based mainly on the electromagnetic calorimeters and the tracking system of the DELPHI detector [12]. All three major electromagnetic calorimeters in DELPHI, the High density Projection Chamber (HPC), the Forward ElectroMagnetic Calorimeter (FEMC) and the Small angle TIle Calorimeter (STIC), have been used in the single-photon reconstruction. The barrel region is covered by the HPC, which is a gas sampling calorimeter able to sample a shower nine times longitudinally. The FEMC is made up of an array of 4532 lead glass blocks in each endcap. The energy resolution of this calorimeter is degraded by the material in front of it, which causes photon conversions and even preshowers. The very forward luminosity monitor STIC [13] consists of two cylindrical lead-scintillator calorimeters read out by wavelength-shifting fibres. Two layers of scintillators mounted on the front of each STIC calorimeter

together with a smaller ringshaped scintillator mounted directly on the beampipe, provide $e - \gamma$ separation. The angular coverages of these calorimeters and the energy resolutions are given in Table 1 and the detailed characteristics and performances are described in [12].

Three different triggers are used in DELPHI to select single-photon events. The HPC trigger for purely neutral final states uses a plane of scintillators inserted into one of the HPC sampling gaps at a depth of around 4.5 radiation lengths. A second level trigger decision is produced from the signals of analog electronics and is based on a coincidence pattern inside the HPC module. The trigger efficiency has been measured with Compton and Bhabha events. It is strongly dependent on the photon energy, E_γ, rising steeply up to ∼12 GeV, with about 30% efficiency at 4 GeV and above 80% when $E_\gamma > 30$ GeV. It reaches a maximum of 87% at $E_\gamma \simeq E_{\text{beam}}$. This efficiency does not include losses due to the cracks between modules of the HPC detector. The FEMC trigger requires an energy deposition of at least 2.5 GeV. The efficiency increases with energy and is ∼97% at 18 GeV. Correlated noise in several adjacent channels causes fake triggers, but these can be rejected offline with high efficiency by algorithms that take into account the lead glass shower pattern. The STIC trigger requires an energy deposition of at least 15 GeV and reaches maximum efficiency at 30 GeV. The trigger efficiency has been measured with samples of photons from $e^+e^-\gamma$ and $q\bar{q}\gamma$ events. The efficiency varied between 74% and 27% over the angular region used in the analysis.

In addition to the electromagnetic calorimeters, the DELPHI tracking system was used to reject events in which charged particles are produced. The main tracking devices are the Time Projection Chamber (TPC) and the microVertex silicon Detector (VD) and its extension into the forward region, the Very Forward Tracker (VFT). The silicon trackers are also used for electron/photon separation by vetoing photon candidates which can be associated with hits in these detectors.

Finally, the Hadron CALorimeter (HCAL) and its cathode-read-out system were used to reject cosmic rays and to provide photon/hadron separation, while the DELPHI Hermeticity Taggers were used to ensure complete detector hermeticity for additional neutral particles.

	Type	Angular coverage	σ_E/E	X_0
STIC:	Lead/scint.	$2° < \theta < 10°$, $170° < \theta < 178°$	$0.0152 \oplus (0.135/\sqrt{E})$	27
FEMC:	Lead glass	$10° < \theta < 37°$, $143° < \theta < 170°$	$0.03 \oplus (0.12/\sqrt{E}) \oplus (0.11/E)$	20
HPC:	Lead/gas	$40° < \theta < 140°$	$0.043 \oplus (0.32/\sqrt{E})$	18

Table 1: Polar angle coverage, energy resolution (where E is in GeV and $\oplus$ denotes addition in quadrature) and thickness (in radiation lengths) of the electromagnetic calorimeters in DELPHI.

3 Event selection

3.1 Single-photon events

The basic selection criteria of events were the same for the three electromagnetic calorimeters: no charged particle tracks detected and no electromagnetic showers apart

from the tracks and showers caused by the single-photon candidate. However, the details of the selection varied somewhat for the different electromagnetic calorimeters:

- Events with a photon in the HPC were selected by requiring a shower having an energy above 6 GeV and a polar angle, θ, between 45° and 135° and no charged particle tracks. The shower was required to satisfy conditions defining a good electromagnetic shape [4]. Background from radiative Bhabha events and Compton events were rejected by requiring no other electromagnetic showers in the event unless they were in the HPC and within 20° of the first one. Cosmic rays were rejected mainly by the hadron calorimeter. If there were two or more hadronic showers the event was discarded and if only one HCAL shower was present, the event was rejected if the shower was not consistent with being caused by punch-through of the electromagnetic shower. A constraint on the γ direction was imposed, requiring that the line of flight from the mean interaction point and the shower direction measured in the calorimeter coincided within 15°. Also the requirement of no charged particles removed cosmic ray background. The photon identification efficiency depended on the criteria applied to require a good electromagnetic shower. It was determined on the basis of a Monte Carlo sample of events passed through the complete simulation of the DELPHI detector [14]. The efficiency also depended on the photon energy and it ranged from ∼45% at 6 GeV to ∼71% for $E_\gamma > 15$ GeV.

- Events with at least one shower in the FEMC with an energy above 18 GeV and a polar angle in the intervals $12° < \theta < 32°$ or $148° < \theta < 168°$ were also selected. Showers in the inner and outer radial parts of the FEMC were discarded because of the large amount of material (about $2X_0$) in front of the FEMC due to the STIC and the TPC detectors. In order to separate electrons from photons, the FEMC shower was extrapolated to the interaction point and the event was rejected if hits in the silicon microvertex detectors (VD and VFT) could be associated with the shower.

  The material in front of the FEMC meant that about half of the photons preshowered before reaching the calorimeter. Most of the preshower was contained in a cone of about 15° around the largest shower and the selection took this into account by requiring no charged particle tracks, no other electromagnetic showers and no hadronic showers outside a 15° cone. If there were no charged particle tracks inside the cone either, i.e., the photon had not preshowered, it was required that only one FEMC shower was present in the event. If, on the other hand, charged particle tracks were present in the cone, more FEMC showers were allowed and their momentum vectors were added to that of the largest shower.

  The requirement of no electromagnetic showers outside the cone greatly reduced the background of radiative Bhabha and Compton events by rejecting events that had one or both electrons in the acceptance of the experiment. Events due to cosmic rays were rejected by the requirement of no hadronic showers outside the cone. Inside the cone, hadronic energy was allowed only in the first layer of the HCAL.

  Most reconstruction and event selection efficiencies in the analysis were taken into account by using Monte Carlo samples passed through the extensive detector simulation package of DELPHI [14]. Some efficiencies, however, were determined from data. In particular, the requirements of no electromagnetic or hadronic showers and no charged particles were studied. A sample of events triggered at random and a sample of back-to-back Bhabha events with the electrons in the STIC were used for this purpose. It was found that noise and machine background caused showers and tracks which would veto about 14% of the good single-photon events.

- Single photons in the STIC were preselected by requiring one shower with an energy of at least 27 GeV in one of the two STIC calorimeters and with $3.8° < \theta < 8°$ or $172° < \theta < 176.2°$ and no other electromagnetic showers, no hadronic showers and no charged particles in the event. It was furthermore required that all single-photon candidates had satisfied the STIC single-photon trigger and that there was no signal in at least one of the two scintillator planes in front of the shower. A requirement of no signal in the small scintillators mounted on the beampipe made it possible to reject some of the radiative $ee\gamma$ background. In spite of the scintillator requirements, the huge background of off-energy electrons made it necessary to introduce a θ-dependent energy cut in such a way that $x_\gamma > (9.2° - \theta)/9°$ for $\theta < 6.5°$ where $x_\gamma = E_\gamma/E_{beam}$.
  The trigger efficiency in the STIC acceptance was discussed in Section 2. The offline photon identification and reconstruction resulted in an additional loss of 5% of the photons. The selection of events with no shower in the STIC and no tracks implied similar losses to those found in the FEMC analysis and were estimated with the same methods.

3.2   Non-pointing single-photon events

The fine granularity of the HPC calorimeter provided a precise reconstruction of the axis direction in electromagnetic showers. This feature was used to select events with a single photon whose flight direction did not point to the beam interaction region. Events with a single non-pointing photon are expected when two neutral particles with large mean decay paths (> 4 m) are produced which subsequently decay into a photon and an invisible particle.

Events of this kind were searched for by requiring one photon in the HPC calorimeter with $E_\gamma > 10$ GeV and impact parameter exceeding 40 cm. Cosmic ray events, which represent the main experimental background, were largely reduced by vetoing on isolated hits or tracks in the Hermeticity Taggers and signals from the cathode-read-out system of the hadron calorimeter. More details on the precise event selection can be found in [11], where the analysis of the data samples collected at centre-of-mass energies up to 183 GeV is described. The same analysis has been applied to the data sample taken at 189 GeV.

3.3   Multi-photon events

A study of final states with at least two photons and missing energy at $\sqrt{s} = 189$ GeV has also been made.

As for non-pointing single photons, the physics motivations and the selection criteria have been discussed in detail in the published paper [11] dedicated to the analysis of the data taken at centre-of-mass energies up to 183 GeV. Here only a brief update of the results is given using the 189 GeV data and the same analysis method.

The selection of multi-photon final states was, as in the 183 GeV analysis, based on a two-step procedure:

- In a first step all events with missing transverse energy and at least two photons, each with $x_\gamma > 0.05$ (where $x_\gamma = E_\gamma/E_{beam}$), were preselected. Very loose cuts on the polar angle of the photon and acoplanarity were adopted for the selection of this sample, which was used to monitor the modelling of the $e^+e^- \to \nu\nu\gamma\gamma(\gamma)$ process by the KORALZ 4.02 generator [15].

- In a second step these criteria were tightened in order to improve the experimental sensitivity for possible signals of supersymmetry, such as the $e^+e^- \to \tilde{\chi}_1^0 \tilde{\chi}_1^0 \to \tilde{G}\gamma\tilde{G}\gamma$ or $e^+e^- \to \tilde{\chi}_2^0 \tilde{\chi}_2^0 \to \tilde{\chi}_1^0 \gamma \tilde{\chi}_1^0 \gamma$ processes. This was achieved by imposing more stringent requirements on the photon polar angles as well as on the event missing mass and transverse momentum.

More details on the event selection can be found in [11].

4 Real and simulated data samples

Apart from the $e^+e^- \to \nu\bar{\nu}\gamma(\gamma)$ process, single-photon events can be faked by the QED reaction $e^+e^- \to e^+e^-\gamma$ if the two electrons escape undetected along the beampipe or if the electrons are in the detector acceptance but are not detected by the experiment.

This process has a very high cross-section, decreasing rapidly when the energy (E_γ) and the polar angle (θ_γ) of the photon increase. The behaviour of this QED background together with the rapidly varying efficiencies at low energies are the reasons why different energy cuts had to be applied for photons in the three calorimeters. In the final analysis it was required that $x_\gamma > 0.06$ (HPC) and $x_\gamma > 0.2$ (FEMC). In the STIC analysis, the requirement was $x_\gamma > 0.3$ for $6.5° < \theta < 8.0°$ and $x_\gamma > (9.2° - \theta)/9°$ for $3.8° < \theta < 6.5°$.

The critical parameter in the rejection of the $e^+e^-\gamma$ background is the polar angle at which the electrons start being seen in the STIC detector. This detector reconstructs electrons down to $\theta = 2.2°$ and in addition, the scintillator counters mounted on the beampipe can be used to reject events with electrons down to $1.8°$. Simulations have shown that even at lower angles (down to $0.97°$) a large fraction of the electrons are detectable because they interact with a tungsten shield mounted inside the beampipe and leak enough energy into the STIC to make it possible to reject the events.

The remaining background from the $e^+e^-\gamma$ process was calculated with a Monte Carlo program [16] and two different event topologies were observed. Either both electrons were below the STIC acceptance or one of the electrons was in the DELPHI acceptance where it was wrongly identified as a photon, and the photon was lost in the cracks between the electromagnetic calorimeters. The first topology gives background at low photon energy while the second one produces fake photon events at high energy. In the HPC acceptance an analytical calculation [17] was also used to confirm that the $e^+e^-\gamma$ background was negligible.

In the STIC analysis, an additional background is the single electrons produced by interactions between the beam particles and residual gas molecules in the LEP beampipe. In these $e \to e\gamma$ events the photons are always lost in the beampipe while the off-energy electrons are bent into the STIC acceptance by the low-beta quadrupoles close to DELPHI. The rate of this background is so large that it was not possible to provide a $\gamma-e$ separation powerful enough to eliminate this background completely. A simulation has been made of off-energy electron production [18], but it could not be used in the analysis since the vacuum pressure around the LEP ring was not known to the required precision. Instead, a background sample was collected with a trigger similar to the photon trigger except that it did not use the scintillators for photon-electron separation. After applying all the cuts used in the single photon analysis, except the scintillator requirements, this background sample was used to estimate the remaining off-energy electron background.

The contribution from other processes such as $\gamma\gamma$ collisions, $e^+e^- \to \gamma\gamma\gamma$, cosmic ray events, $e^+e^- \to \mu^+\mu^-\gamma$ and $e^+e^- \to \tau^+\tau^-\gamma$ has also been calculated.

The $\nu\bar{\nu}\gamma(\gamma)$ process was simulated by both the KORALZ [15] and the NUNUGPV [19] program with very similar results (the numbers of expected events in the HPC region at 189 GeV were estimated to be 156.8 and 157.7 with the two programs respectively).

A detailed discussion on the backgrounds for the non-pointing single-photon events and for the multi-photon events is contained in [11].

	HPC		FEMC		STIC	
θ_γ:	$45° - 135°$		$12° - 32°$, $148° - 168°$		$3.8° - 8.0°$, $172° - 176.2°$	
x_γ:	> 0.06		0.2 - 0.9		0.3 - 0.9	
$\sqrt{s}$:	182.7 GeV	188.7 GeV	182.7 GeV	188.7 GeV	182.7 GeV	188.7 GeV
Luminosity:	$50.2\ pb^{-1}$	$154.7\ pb^{-1}$	$49.2\ pb^{-1}$	$157.7\ pb^{-1}$	$51.4\ pb^{-1}$	$157.3\ pb^{-1}$
$N_{observed}$:	54	146	65	155	32	94
$N_{background}$:	0.08	0.3	3.5	6.0	3.6	6.5
$N_{e^+e^-\to\nu\bar{\nu}\gamma}$:	59.5±1.6	156.8±4.3	55.0±1.2	153.4±1.9	32.4±0.7	91.4±0.9
σ_{meas} (pb)	1.85±0.25	1.80±0.15	2.33±0.31	1.89±0.16	1.27±0.25	1.41±0.15
$\sigma_{\nu\bar{\nu}\gamma(\gamma)}$ (pb)	2.04	1.97	2.08	1.94	1.50	1.42
N_ν	2.63±0.49	2.65±0.31	3.42±0.51	2.91±0.28	2.49±0.57	2.98±0.37

Table 2: Number of selected and expected single photon events, measured and calculated cross-section for $e^+e^- \to \nu\bar{\nu}\gamma(\gamma)$ (KORALZ with three neutrino generations) and the number of neutrino generations calculated from the cross-sections. The errors are statistical only. x_γ is E_γ/E_{beam}.

	HPC		FEMC		STIC	
Source	Variation	$\Delta\sigma$	Variation	$\Delta\sigma$	Variation	$\Delta\sigma$
Luminosity	±0.6%	±0.6%	±0.6%	±0.6%	±0.6%	±0.6%
Trigger efficiency	±5%	±5%	±2%	±2%	±6%	±6%
Identification efficiency	±5%	±5%	±6%	±6%	±5%	±5%
Calorimeter energy scale	±5%	±4%	±4%	±4%	±0.5%	±1%
Background	±57%	±0.1%	±55%	±2%	±62%	±5%
Total		±8%		±8%		±9%

Table 3: Contributions to systematic error. The total systematic error is the quadratic sum of the individual errors.

5 Comparison with the Standard Model expectations

5.1 Single-photon cross-section

The final numbers of expected and observed single-photon events are given in Table 2 and the x_γ spectrum of the selected events at 189 GeV is shown in Figure 1 together with the expected background and the $\nu\bar{\nu}\gamma$ contribution. The single-photon event selection was such that events with more than one photon could survive if the other photons were
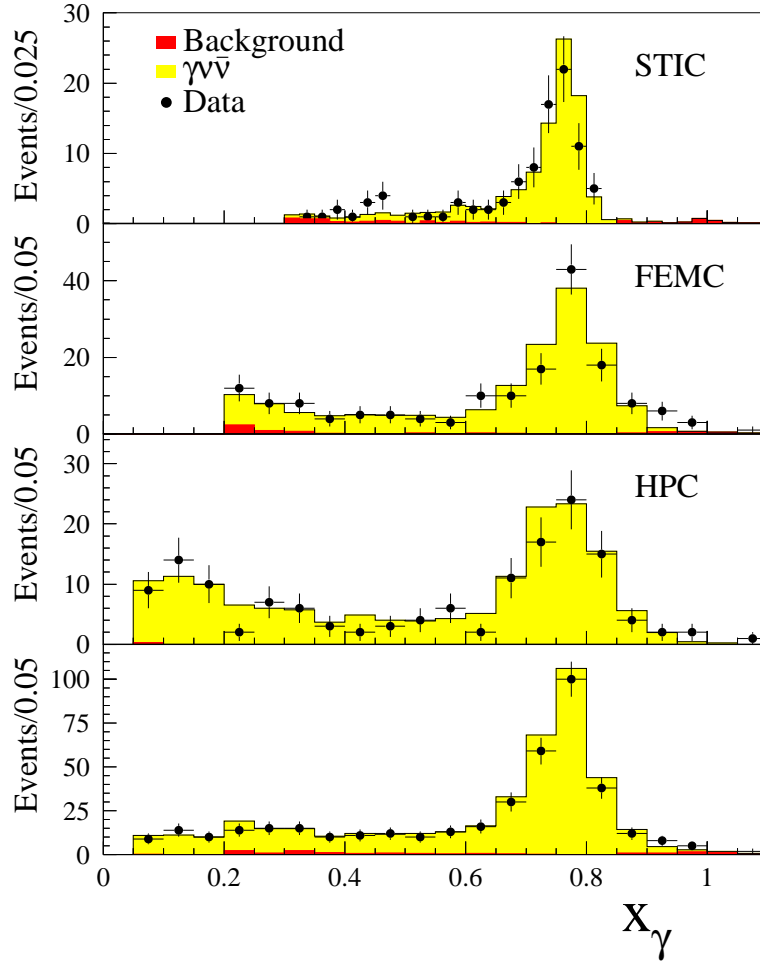
Figure 1: x_γ of selected single photons at 189 GeV in the three calorimeters STIC, FEMC and HPC. The bottom plot shows the combined spectrum. The light shaded area is the expected distribution from $e^+e^- \to \nu\bar{\nu}\gamma$ and the dark shaded area is the total background from other sources.

at low angle ($\theta_\gamma < 2.2°$), low energy ($E_\gamma < 0.8$ GeV) or within 3°, 15° and 20° from the highest energy photon in the STIC, FEMC and HPC respectively. In total, 546 single-photon events were observed at 189 GeV and 183 GeV in the three calorimeters, with 570 events expected from known sources.

The measured cross-sections calculated from the single-photon events after correcting for background and efficiencies are given in Table 2. The previously mentioned Monte Carlo programs were used to calculate the expected values of the cross-section of the process $e^+e^- \to \nu\bar{\nu}\gamma(\gamma)$ inside the acceptance of each of the three detectors used in the analysis. Figure 2 shows the expected behaviour of the cross-section, calculated with NUNUGPV for three neutrino generations, compared with the values measured with the HPC detector at different LEP energies. The contributions from various sources to the systematic error in the cross-section measurement are given in Table 3. The dominant uncertainty comes from the estimation of trigger and detection efficiencies. The calculation of the expected cross-section has a theoretical uncertainty which is approaching 1% with the latest versions of NUNUGPV [19] and KORALZ [15] and this error is thus insignificant compared with the experimental systematic errors.

A measurement of the cross-section of the process $e^+e^- \rightarrow \nu\bar{\nu}\gamma$ determines the number of light neutrino generations, N_ν. DELPHI has previously reported a value of $N_\nu = 2.89 \pm 0.32$ from LEP1 single photon data [20]. The LEP2 cross-section measurements have now been compared with the expected cross sections for 2, 3 and 4 neutrino generations, calculated with KORALZ, and the number of neutrino generations has been deduced (Table 2). Averaging the three independent measurements from the three different calorimeters at 183 GeV and 189 GeV, the number of light neutrino generations becomes:

$$N_\nu = 2.84 \pm 0.15(stat) \pm 0.14(syst)$$
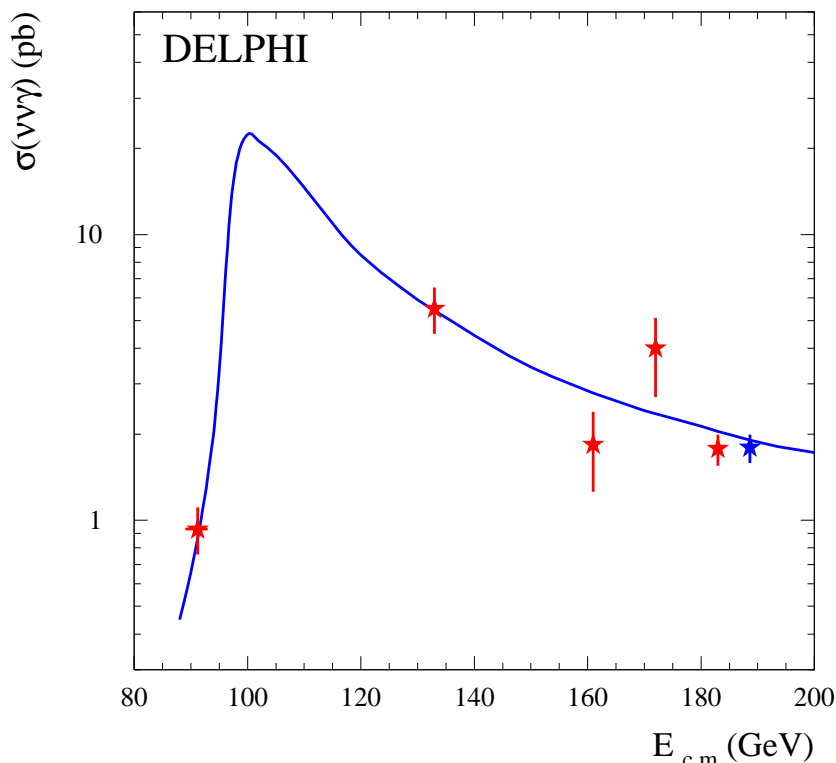
Figure 2: The measured cross-sections in the HPC for $E_\gamma > 6$ GeV at different $\sqrt{s}$ compared to the expected $\sigma(\nu\bar{\nu}\gamma)$ (for three neutrino generations).

5.2 Non-pointing single-photon events and multi-photon events

The numbers of events with a single non-pointing photon or with multi-photon final states found in the data sample at 189 GeV are compared to Standard Model expectations in Table 4.

The missing mass spectra for the preselected multi-photon events and the expected contribution from $e^+e^- \rightarrow \nu\bar{\nu}\gamma\gamma(\gamma)$ as simulated with KORALZ are shown in Figure 3. The measured missing mass distribution is in good agreement with the simulation.

No excess over Standard Model expectations was found in any of the data samples collected at $\sqrt{s} = 189$ GeV. Hence these data were combined with lower energy data to extract limits on new physics.

	189 GeV		130-189 GeV	
	Observed	Expected	Observed	Expected
Preselected multi-photon events	17	15.1±0.9	27	25.3±1.0
$e^+e^- \to \tilde{\chi}_1^0\tilde{\chi}_1^0 \to \tilde{G}\gamma\tilde{G}\gamma$ selection	5	4.4±0.5	7	7.1±0.5
$e^+e^- \to \tilde{\chi}_2^0\tilde{\chi}_2^0 \to \tilde{\chi}_1^0\gamma\tilde{\chi}_1^0\gamma$ selection	8	5.2±0.5	12	8.6±0.6
Non-pointing single-photon events	4	5.0±0.6	6	7.6±0.9

Table 4: The number of observed and expected events from Standard Model sources in four selected data samples.
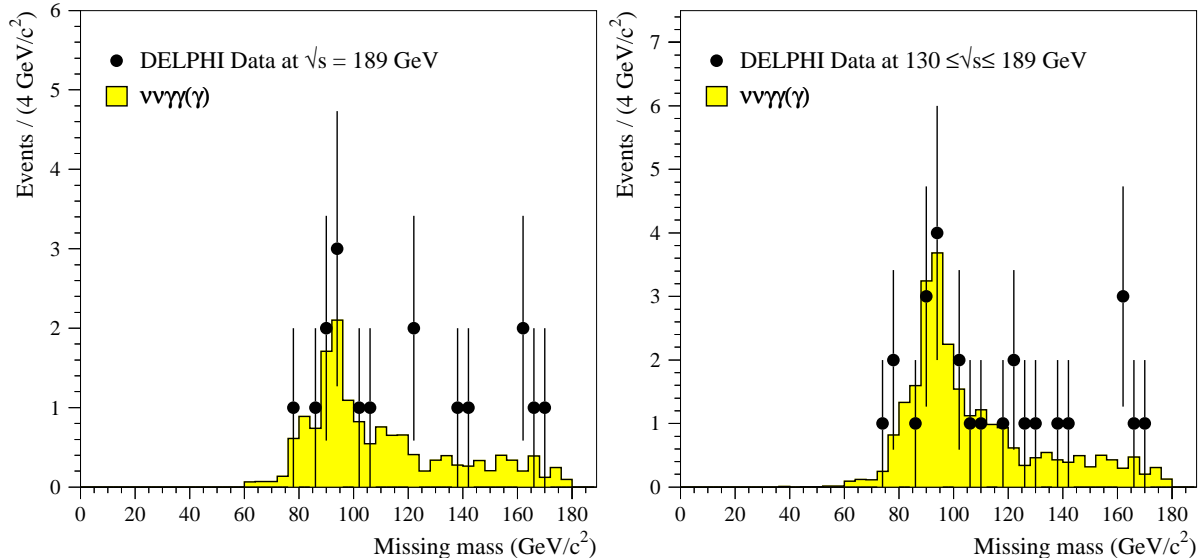
Figure 3: Missing mass distribution observed after multi-photon preselection in the 189 GeV sample (left) and the combined 130-189 GeV sample (right).

6 Limits on new phenomena

6.1 Limits on the production of an unknown neutral state

In many previous analyses [4,20,21] the observed single-photon candidates have been used to set a limit on the probability of the existence of a new particle, X, produced in association with a photon and being stable or decaying into invisible particles. The limit is calculated from the missing mass distribution (Figure 4) of the 395 single photon events at 189 GeV in the γ angular region $3.8° < \theta < 176.2°$, while taking into account the expected contributions from the Standard Model. The limit is valid when the intrinsic width of the X particle is negligible compared with the detector resolution (the missing mass resolution varies between 10 GeV/c^2 at the Z^0 peak to 1 GeV/c^2 at high masses).
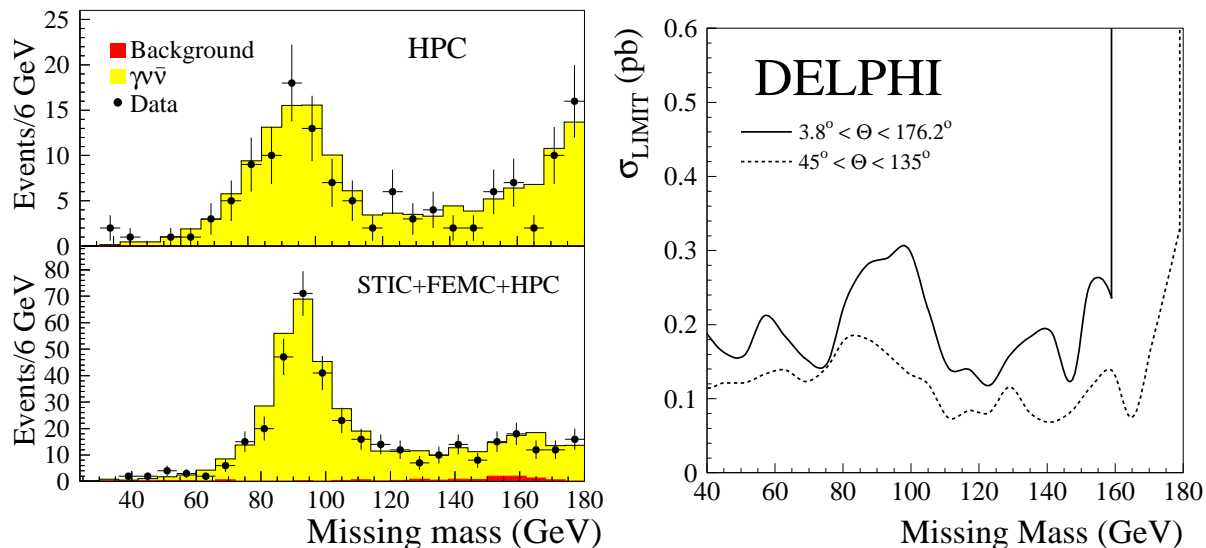
Figure 4: Left: The distributions of the missing mass for the events at 189 GeV in the HPC and in all three calorimeters. The light shaded area is the expected distribution from $e^+e^- \to \nu\bar{\nu}\gamma$ and the dark shaded area is the total background from other sources. Right: upper limit at 95% C.L. (within the solid angles described) for the production of a new unknown stable neutral object .

The upper limit at the 95% confidence level of the cross-section for $e^+e^- \to \gamma + \mathrm{X}$ is given in Figure 4 for photons in the HPC region and in all three calorimeters combined. In the latter case an assumption of an ISR-like photon angular distribution has been made to correct for the regions between the calorimeters.

6.2   Limits on the production of gravitons

It has been suggested recently [8,9] that gravitational interactions could be unified with gauge interactions already at the weak scale if there are extra compact dimensions of space in which only gravity can propagate. The observed weakness of gravitation compared to other forces would be related to the size of the compactified extra dimensions. A fundamental mass scale M_D is introduced, which is related to the gravitational constant G_N and to the size or radius R of the compactified space (assumed to be a torus) by

$$M_D^{n+2} R^n = (8\pi G_N)^{-1}$$

where n is the number of dimensions in addition to the usual 4 dimensional space. With one extra dimension and a fundamental scale of 0.5-1 TeV, the size of this dimension becomes $10^{12} - 10^{13}$ m which is excluded by macroscopic measurements. However, already with two extra dimensions, R is in the range 0.5-1.9 mm and with n=6 the size of the dimensions becomes 0.3-0.7 Å. In this case the modification of the gravitational force would not have been observed in previous gravitational measurements.

The consequence of this model is that at LEP gravity could manifest itself by the production of gravitons (G), which themselves would be undetectable by the experiments. Instead single photons from the $e^+e^- \to \gamma G$ reaction are observable. The differential cross-section for this process has been calculated [9]. Most of the signal is expected at low photon energy and, since $\sigma \sim s^{n/2}/M_D^{n+2}$, at the highest available centre-of-mass
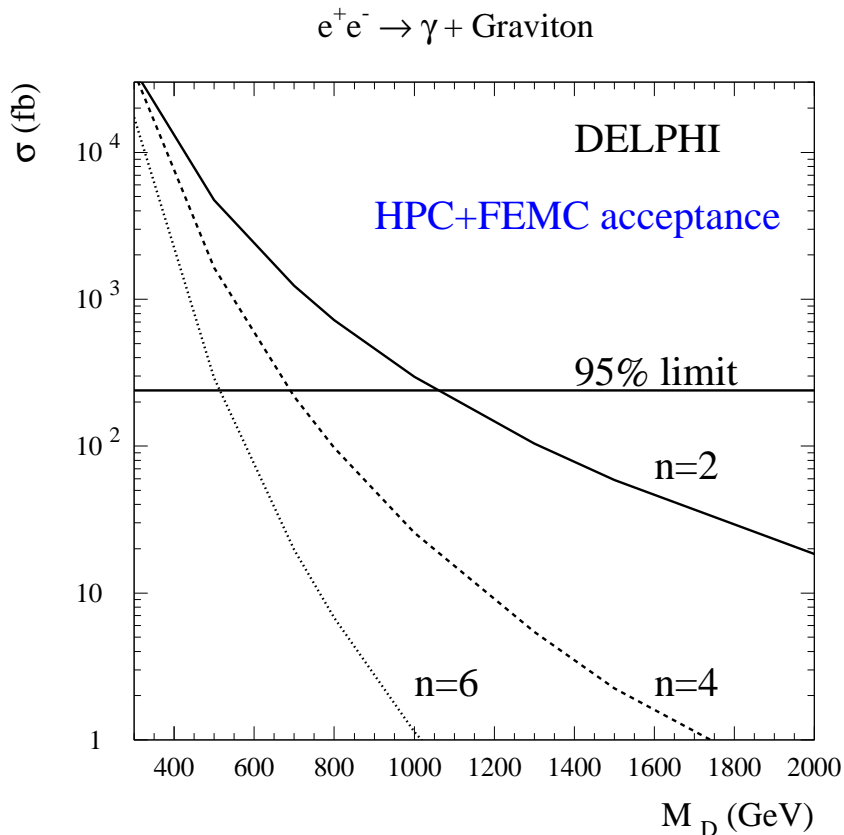
$$e^+e^- \rightarrow \gamma + \text{Graviton}$$

Figure 5: The cross-section limit at 95% C.L. for $e^+e^- \rightarrow \gamma G$ production and the expected cross-section for 2, 4 and 6 extra dimensions.

energy. For this reason, only the HPC and the FEMC data recorded at 189 GeV were used to set a limit on the gravitational scale. After the sensitivity had been optimised for each calorimeter, the single photon sample consisted of 59 events with a photon in the HPC with $6 < E_\gamma < 50$ GeV and 45 events with a photon in the FEMC with $18 < E_\gamma < 50$ GeV. The numbers of events expected in the Standard Model were 64 and 41 for the two calorimeters respectively. A cross-section limit of

$$\sigma < 0.24 \text{ pb} \quad \text{at } 95\% \text{ C.L.} \tag{1}$$

results in limits on the fundamental mass scale of $M_D > 1.10$ TeV, $M_D > 0.68$ TeV and $M_D > 0.51$ TeV for 2, 4 and 6 extra dimensions (Figure 5). This translates into a limit on the size of the dimensions of $R < 0.4$ mm for $n = 2$. If the systematic errors are taken into account, the M_D-limit for two extra dimensions is reduced by 9% and the limits for $n = 4$ and 6 by 3%.

6.3 Limits on compositeness

Composite models predict several new particles which do not exist in the Standard Model. A specific Preon Model is considered in this analysis [10]. This model considers leptons, quarks and weak bosons as composite particles. Some of the predicted new particles contribute to the cross-section of the process $e^+e^- \rightarrow \gamma + invisible\ particles$. At a relatively light mass scale, the model predicts the existence of objects connected with
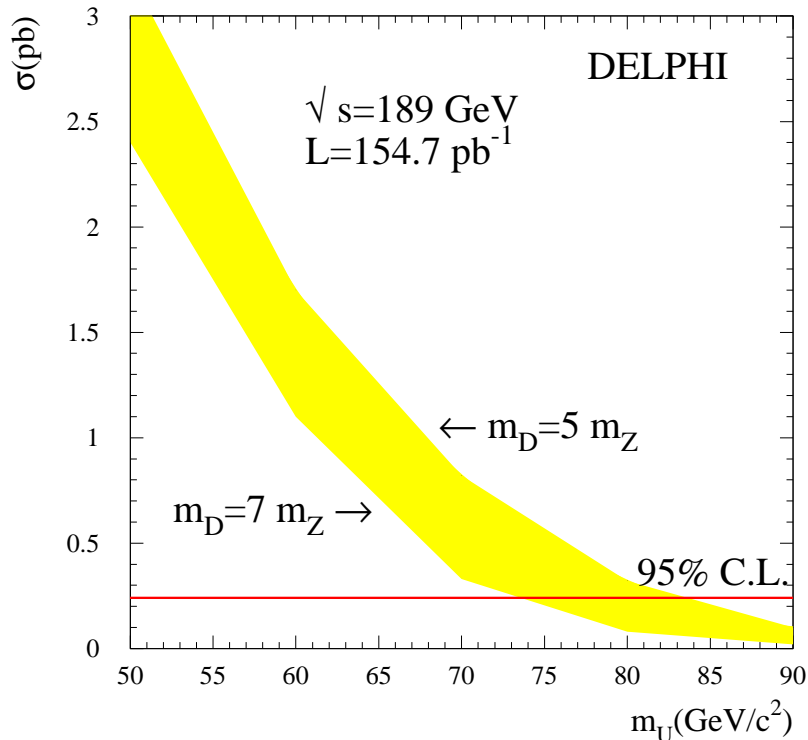
Figure 6: Cross section limit at 95% C.L. for the production of a W-type U boson from 189 GeV data. The shaded area shows the cross-section predicted by the Preon Model described in the text.

neutrinos $(l_S, \bar{l}_S)$, with down quarks (q') and with W bosons $(U^\pm, U^0)$. It also requires a new vector boson D, which could be several times more massive than the Z^0. The U^0 boson decays invisibly and can be produced in the reaction $e^+e^- \to U^0\bar{U}^0\gamma$, contributing to the process $e^+e^- \to \gamma + invisible\ particles$. Also pairs of $l_S\bar{l}_S$ could be produced through $U^\pm$ exchange and contribute to the single-photon final state.

Calculating the cross-sections with the hypothesis that a composite boson D exists with mass between $m_D = 5m_{Z^0}$ and $m_D = 7m_{Z^0}$ and adding the contributions to the cross-sections coming from direct production of $U^0\bar{U}^0$ pairs and the exchange of $U^\pm$, a limit can be obtained on m_U after subtracting the contribution expected from neutrino production in the Standard Model. The cross-section limit calculated from the HPC and the FEMC data was $\sigma < 0.24$ pb at 95% C.L. as in the graviton analysis and this translates into a limit on the U boson mass which ranges between $m_U > 74-84$ GeV/c^2 at 95% C.L. when m_D is varied in the range indicated above (Figure 6). These limits are reduced by 4% if the systematic errors are taken into account. Weaker limits have been determined at lower LEP2 energies [4].

6.4   Limit on the mass of the gravitino

If the assumption is made that the gravitino is the lightest supersymmetric particle (LSP), $e^+e^- \to \tilde{G}\tilde{G}\gamma$ may be the only kinematically accessible supersymmetric process at LEP as discussed and computed in [6]. Lower limits on the mass of a light gravitino have been extracted in other LEP measurements [3], at $p\bar{p}$ machines [22] and by using astrophysical constraints [23] and $(g-2)_\mu$ measurements [24].

To obtain a limit on the gravitino mass ($m_{\tilde{G}}$), the radiative double differential cross-section $d^2\sigma/(dx_\gamma, dcos\theta_\gamma)$ given in [6] for the radiative production ($e^+e^- \to \tilde{G}\tilde{G}\gamma$), was compared with the observed single photon data. The largest sensitivity is obtained with photons at low energy and/or low polar angle. Single photon final states from the Standard Model process $e^+e^- \to \nu\bar{\nu}\gamma$ have angular distributions similar to the signal, while the photon energy spectrum exhibits the enhanced characteristic peak due to the radiative return to the Z^0, at $x_\gamma = 1 - m_Z^2/s$. Therefore, the optimal kinematic region in which to look for the signal is in the low photon energy region, well below the radiative return peak. Since the signal cross-section grows as the sixth power of the centre-of-mass energy, the highest sensitivity is found at the highest beam energy. For this reason, only the data taken at $\sqrt{s} = 189$ GeV with the FEMC and the HPC detectors have been used. The different low energy regions available to the two calorimeters meant that the HPC events dominated the measurement. Combining the two calorimeters, the same limit of $\sigma < 0.24$ pb at 95% C.L. was obtained as in the graviton analysis. This corresponds to a lower limit on the gravitino mass which is

$$m_{\tilde{G}} > 10.0 \cdot 10^{-6} \text{ eV/c}^2 \quad \text{at 95\% C.L.}$$

Since the supersymmetry-breaking scale $|F|^{\frac{1}{2}}$ is related to the gravitino mass by $|F| = \sqrt{\frac{3}{8\pi}/G_N} \cdot m_{\tilde{G}}$, the limit on the scale is $|F|^{\frac{1}{2}} > 204$ GeV. The effect of the systematic uncertainties on the $m_{\tilde{G}}$-limit is to lower it by 5%.
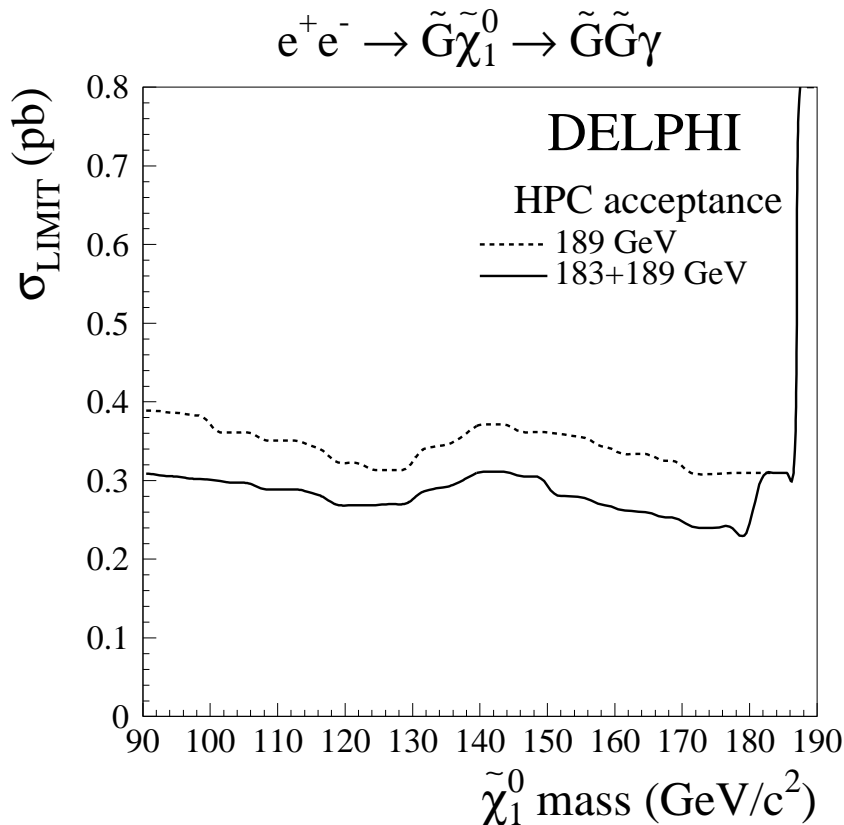
Figure 7: Upper limits for the cross-section of the process $e^+e^- \to \tilde{G}\tilde{\chi}_1^0 \to \tilde{G}\tilde{G}\gamma$ at 95% C.L. The dashed line shows the limit obtained with only the 189 GeV data while the full line represents the combined 183+189 GeV limit after scaling the low energy data to 189 GeV (assuming the signal cross-section to scale as $1/s$).
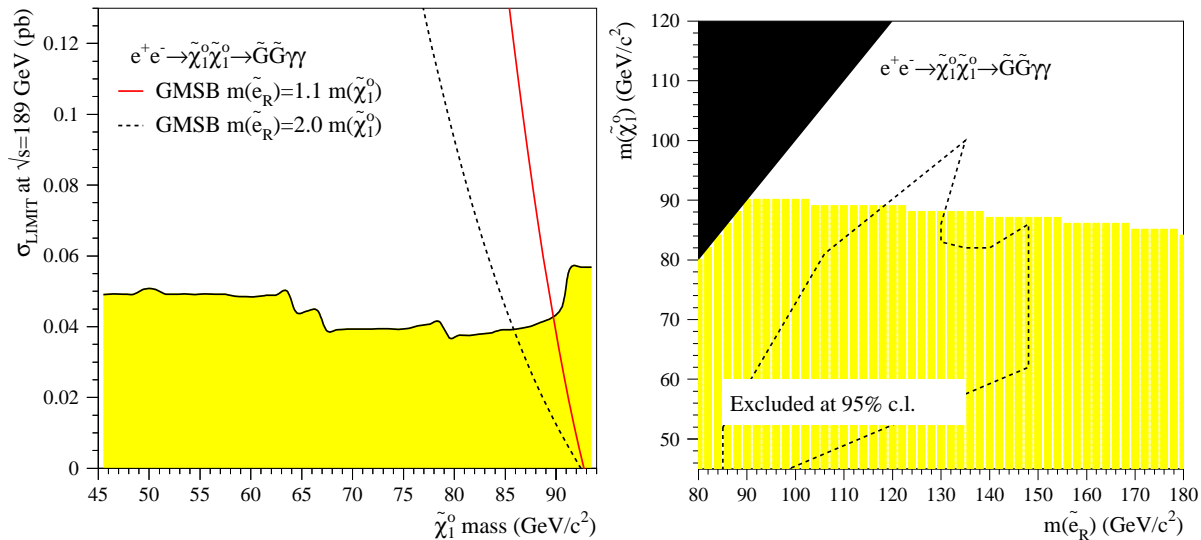
Figure 8: Left: Upper limit at 95% C.L. on the cross-section at $\sqrt{s}$ =189 GeV of the process $e^+e^- \to \tilde{\chi}_1^0\tilde{\chi}_1^0 \to \tilde{G}\gamma\tilde{G}\gamma$ as a function of the $\tilde{\chi}_1^0$ mass and the predicted cross-section for two different assumptions for the selectron mass. The limit was obtained by combining all data taken at $\sqrt{s}$ =130-189 GeV, assuming the signal cross-section scales as β/s (where β is the neutralino velocity). Right: The shaded area shows the exclusion region in the $m_{\tilde{\chi}}$ versus $m_{\tilde{e}_R}$ plane, calculated from the DELPHI data at $\sqrt{s}$ =130-189 GeV. The region compatible with the selectron interpretation [27] of the CDF ee$\gamma\gamma$ event [28] is shown by the dashed line.

6.5 Limits on neutralino production if $\tilde{G}$ is the LSP

Supersymmetric models such as the gauge-mediated supersymmetric (GMSB) model [1] or the "no-scale" supergravity model (also known as the NLZ model) [2] predict that the gravitino $\tilde{G}$ is the lightest supersymmetric particle (LSP). If the next lightest supersymmetric particle (NLSP) is the neutralino $\tilde{\chi}_1^0$, both single-photon and multi-photon production can occur at LEP2 via the processes $e^+e^- \to \tilde{G}\tilde{\chi}_1^0 \to \tilde{G}\tilde{G}\gamma$ and $e^+e^- \to \tilde{\chi}_1^0\tilde{\chi}_1^0 \to \tilde{G}\gamma\tilde{G}\gamma$. While the rate of the former process is proportional to the inverse of the gravitino mass squared, the di-photon process is independent of the gravitino mass. Consequently, the single-photon process is expected to dominate only for very light gravitinos and calculations done with the NLZ model at $\sqrt{s} = 190$ GeV predict that $e^+e^- \to \tilde{G}\tilde{\chi}_1^0 \to \tilde{G}\tilde{G}\gamma$ can be observed only if $m_{\tilde{G}} < 3 \cdot 10^{-5}$ eV/c^2 [2].

The cross-section limit for $e^+e^- \to \tilde{G}\tilde{\chi}_1^0 \to \tilde{G}\tilde{G}\gamma$ was calculated from the energy distribution of the expected events, generated with SUSYGEN [25], and the observed single photon events in the angular region $45° < \theta < 135°$, after taking into account the expected background from $\nu\bar{\nu}\gamma$. The expected photon energy distribution from $\tilde{\chi}_1^0 \to \tilde{G}\gamma$ is increasing with increasing neutralino mass ($m_{\tilde{\chi}}$) and the cut on E_γ was changed with $m_{\tilde{\chi}}$ in such a way as to keep at least 90% of the signal at all masses. The resulting overall efficiency, including both the energy cut and the geometrical acceptance, varied between 55% and 60% for neutralino masses ranging from 50 to 180 GeV/c^2. The calculated upper limit for the cross-section of the process $e^+e^- \to \tilde{G}\tilde{\chi}_1^0 \to \tilde{G}\tilde{G}\gamma$ is given in Figure 7 for the 189 GeV data alone and after combining the 183 and 189 GeV data using a likelihood ratio method [26]. A branching ratio of 100% for the process $\tilde{\chi}_1^0 \to \tilde{G}\gamma$ was assumed. The
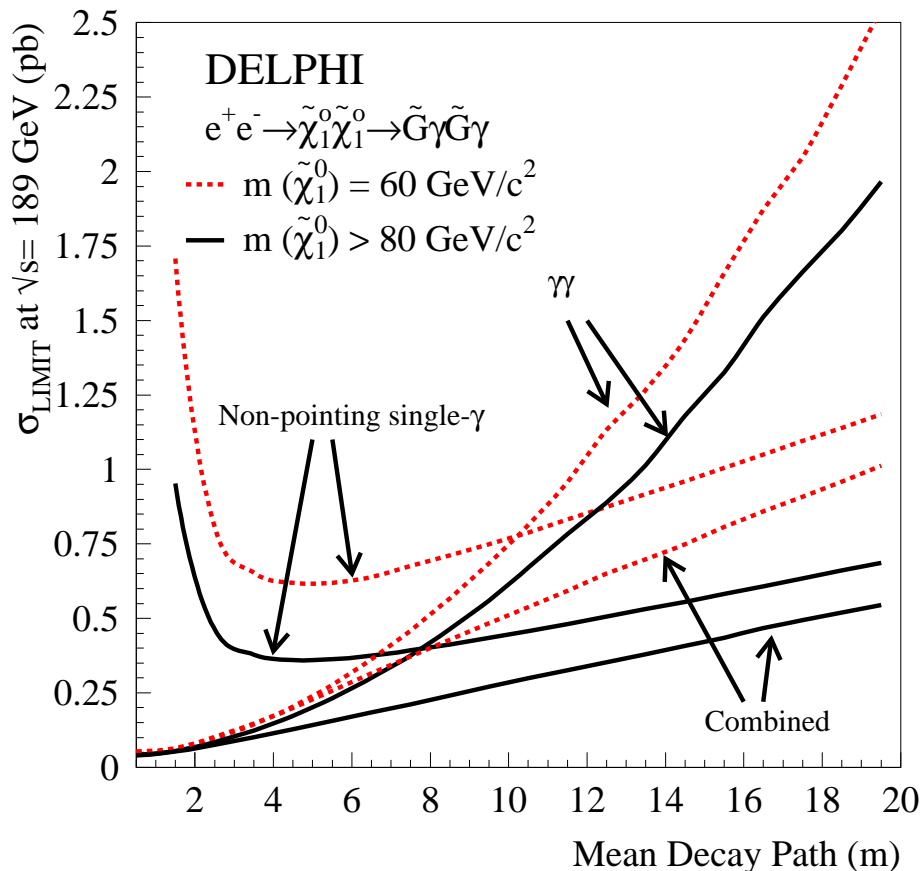
Figure 9: Upper limit at 95% C.L. on the cross-section at $\sqrt{s}$ =189 GeV of the process $e^+e^- \rightarrow \tilde{\chi}_1^0\tilde{\chi}_1^0 \rightarrow \tilde{G}\gamma\tilde{G}\gamma$ as a function of the $\tilde{\chi}_1^0$ mean decay path for two hypotheses for the neutralino mass: $m_{\tilde{\chi}}$ = 60 GeV/c^2 and 80 GeV/c$^2 < m_{\tilde{\chi}} < \sqrt{s}/2$.

measured cross-section limit from the 183+189 GeV (189 GeV) data corresponds to a limit on the neutralino mass of $m_{\tilde{\chi}_1^0} >$ 116 GeV/c^2 (110 GeV/c^2) assuming $m_{\tilde{G}} = 10^{-5}$ eV/c^2 and $m_{\tilde{e}}$ =150 GeV/c^2 [2].

In the search for $e^+e^- \rightarrow \tilde{\chi}_1^0\tilde{\chi}_1^0 \rightarrow \tilde{G}\gamma\tilde{G}\gamma$ at $\sqrt{s}$ =189 GeV, 5 events were observed with 4.4 expected from $e^+e^- \rightarrow \nu\overline{\nu}\gamma\gamma(\gamma)$, which is the dominant Standard Model background. This brings the total number of events found at $\sqrt{s}$ =130-189 GeV to 7 with 7.1 expected (Table 4). Figure 8 shows the cross-section limit [26] calculated from these events as a function of the $\tilde{\chi}_1^0$ mass (assuming a branching ratio of 100% for $\tilde{\chi}_1^0 \rightarrow \tilde{G}\gamma$) and the exclusion region in the $m_{\tilde{\chi}}$ versus $m_{\tilde{e}_R}$ plane. The dependence of the signal cross-section on the selectron mass is due to the possibility of t-channel selectron exchange in the production mechanism. As shown in Figure 8, a lower limit of 86.0 GeV/c^2 (89.5 GeV/c^2) at 95% C.L. for the χ_1^0 mass can be deduced with the hypotheses $m_{\tilde{e}_R} = m_{\tilde{e}_L} = 2m_{\tilde{\chi}}$ ($m_{\tilde{e}_R} = m_{\tilde{e}_L} = 1.1m_{\tilde{\chi}}$) and $\chi_1^0 \approx \tilde{B}$. In the extreme case $m_{\tilde{e}_L} \gg m_{\tilde{e}_R}$, the χ_1^0 mass limit is reduced to 83.5 GeV/c^2 (88.5 GeV/c^2) at 95% C.L.

If the gravitino mass is larger than 200-300 eV/c^2, the $\tilde{\chi}_1^0$ can have such a long lifetime that it will decay far from the production point yet within the detector. The signature for this case is photons that do not point to the interaction region. If the decay length is long, the probability to detect both photons is small and therefore single photon events were searched for which had a shower axis reconstructed in the HPC which gave a beam crossing point at least 40 cm away from the interaction point [11]. Four events were found
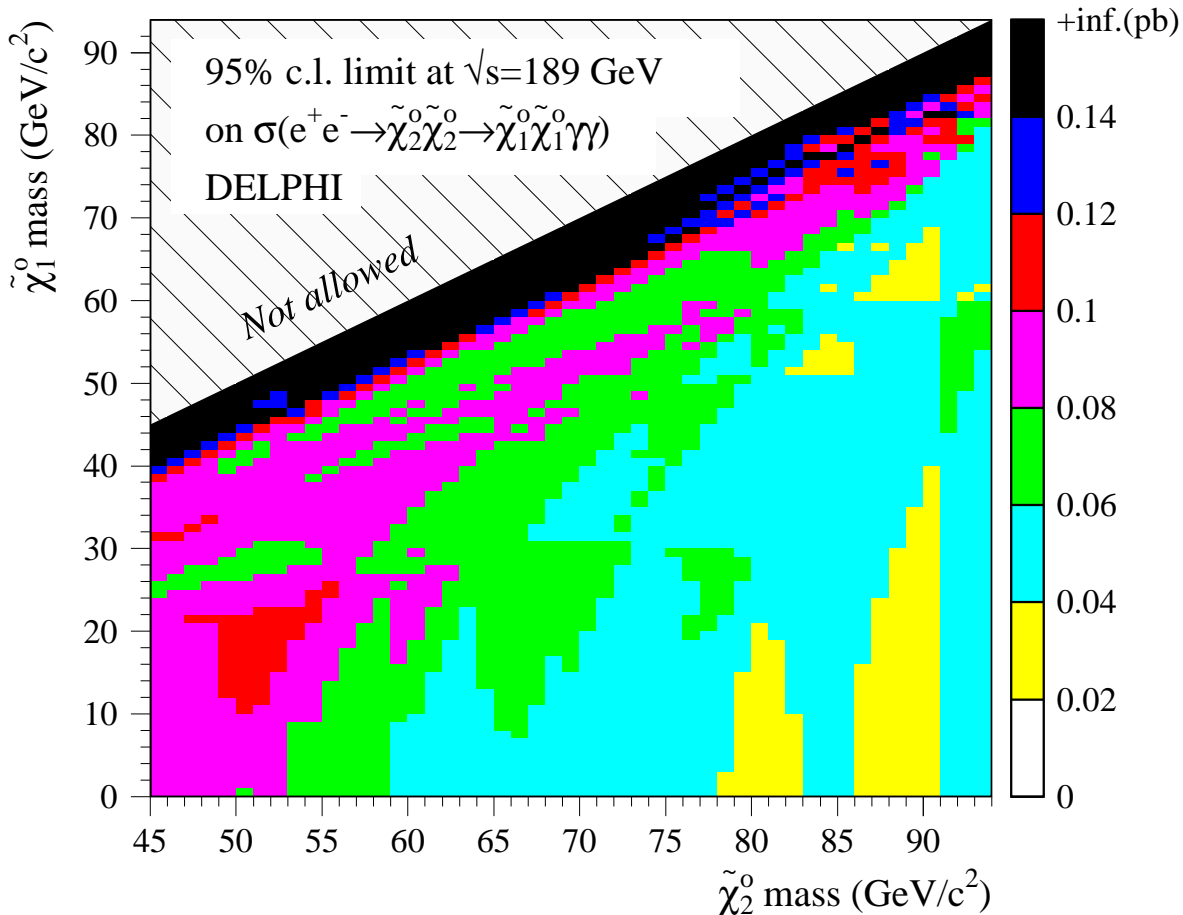
Figure 10: Upper limit at 95% C.L. on the cross-section at $\sqrt{s}$ =189 GeV of the process $e^+e^- \to \tilde{\chi}_2^0\tilde{\chi}_2^0 \to \tilde{\chi}_1^0\gamma\tilde{\chi}_1^0\gamma$ as a function of the $\tilde{\chi}_1^0$ and the $\tilde{\chi}_2^0$ mass. The different shaded areas correspond to limits in pb as indicated by the shading scale on the right hand side. The limit was obtained by combining all data taken at $\sqrt{s}$ =130-189 GeV, assuming the signal cross-section to scale as β/s.

at 189 GeV with 5.2 expected, bringing the total at all energies to 6 with 7.9 expected from Standard Model sources (Table 4).

Figure 9 shows the cross-section limit as a function of the mean decay path of the neutralino using both the multi-photon events and the non-pointing single photon events.

6.6 Limits on neutralino production if $\tilde{\chi}_1^0$ is the LSP

In other SUSY models [7] the $\tilde{\chi}_1^0$ is the LSP and $\tilde{\chi}_2^0$ is the NLSP. The $e^+e^- \to \tilde{\chi}_2^0\tilde{\chi}_2^0 \to \tilde{\chi}_1^0\gamma\tilde{\chi}_1^0\gamma$ process has an experimental signature which is the same as for $e^+e^- \to \tilde{\chi}_1^0\tilde{\chi}_1^0 \to \tilde{G}\gamma\tilde{G}\gamma$ but with somewhat different kinematics due to the masses of the $\tilde{\chi}_1^0$ and the $\tilde{\chi}_2^0$. The previous DELPHI analysis at lower energies [11] has now been repeated with the 189 GeV data sample. Eight events remain after all cuts, with 5.2 expected from the Standard Model background (Table 4). Figure 10 shows the cross-section limit calculated from the events collected at all energies as a function of the $\tilde{\chi}_1^0$ and $\tilde{\chi}_2^0$ masses, assuming a branching ratio of 100% for $\tilde{\chi}_2^0 \to \tilde{\chi}_1^0\gamma$.

7   Conclusions

With the 209 pb^{-1} of data collected by DELPHI in 1997 and 1998 at centre-of-mass energies of 183 GeV and 189 GeV, a study has been made of the production of events with a single photon in the final state and no other visible particles. Previous results on single non-pointing photons and on multi-photon final states have also been updated with 189 GeV data.

The measured single-photon cross-sections are in agreement with the expectations from the Standard Model process $e^+e^- \to \nu\bar{\nu}\gamma$ and the number of light neutrino families is measured to be:

$$N_\nu = 2.84 \pm 0.15(stat) \pm 0.14(syst)$$

The absence of an excess of events with one or more photons in the final state has been used to set limits on the production of a new unknown model-independent neutral state, a W-type U-boson as described by a composite model, gravitons propagating in high-dimensional space, a light gravitino and neutralinos.

References

[1] S. Dimopoulos *et al.*, Phys. Rev. Lett. **76** (1996) 3494;
S. Dimopoulos *et al.*, Nucl. Phys. **B488** (1997) 39;
S. Ambrosanio *et al.*, Phys. Rev. **D54** (1996) 5395;
S. Ambrosanio *et al.*, Phys. Rev. **D56** (1997) 1761.

[2] J. L. Lopez *et al.*, Phys. Rev. Lett. **77** (1996) 5168;
J. L. Lopez *et al.*, Phys. Rev. **D55** (1997) 5813.

[3] ALEPH Collaboration, R. Barate *et al.*, Phys. Lett. **B420** (1998) 127;
ALEPH Collaboration, R. Barate *et al.*, Phys. Lett. **B429** (1998) 201;
L3 Collaboration, M. Acciarri *et al.*, Phys. Lett. **B411** (1997) 373;
L3 Collaboration, M. Acciarri *et al.*, Phys. Lett. **B444** (1998) 503;
L3 Collaboration, M. Acciarri *et al.*, Phys. Lett. **B470** (1999) 268;
OPAL Collaboration, K. Ackerstaff *et al.*, Eur. Phys. J. **C2** (1998) 607;
OPAL Collaboration, K. Ackerstaff *et al.*, Eur. Phys. J. **C8** (1999) 23.

[4] DELPHI Collaboration, P. Abreu *et al.*, Phys. Lett. **B380** (1996) 471.

[5] DELPHI Collaboration, P. Abreu *et al.*, Eur. Phys. J. **C1** (1998) 1.

[6] A. Brignole, F. Feruglio and F. Zwirner, Nucl. Phys. **B516** (1998) 13;
A. Brignole, F. Feruglio and F. Zwirner, Erratum-ibid. **B555** (1999) 653.

[7] S. Ambrosanio and B. Mele, Phys. Rev. **D52** (1995) 3900;
S. Ambrosanio and B. Mele, Phys. Rev. **D53** (1996) 2541;
S. Ambrosanio *et al.*, Nucl. Phys. **B478** (1996) 46;
S. Ambrosanio and B. Mele, Phys. Rev. **D55** (1997) 1392;
G.L. Kane and G. Mahlon, Phys. Lett. **B408** (1997) 222.

[8] N. Arkani-Hamed, S. Dimopoulos and G. Dvali, Phys. Lett. **B429** (1998) 263.
E.A. Mirabelli, M. Perelstein and M.E. Peskin, Phys. Rev. Lett. **82** (1999) 2236.

[9] G.F. Giudice, R. Rattazzi and J.D. Wells, Nucl. Phys. **B544** (1999) 3.

[10] H. Senju, Prog. Theor. Phys. **95** (1996) 455 and references therein.

[11] DELPHI Collaboration, P. Abreu *et al.*, Eur. Phys. J. **C6** (1999) 371.

[12] DELPHI Collaboration, P. Aarnio *et al.*, Nucl. Inst. and Meth. **A303** (1991) 233;
DELPHI Collaboration, P. Abreu *et al.*, Nucl. Inst. and Meth. **A378** (1996) 57.

[13] S.J. Alvsvaag *et al.*, Nucl. Inst. and Meth. **A425** (1999) 106.

[14] DELPHI Collaboration, DELPHI 89-67 PROG 142;
DELPHI Collaboration, DELPHI 89-68 PROG 143.

[15] S. Jadach *et al.*, Comp. Phys. Comm. **66** (1991) 276;
S. Jadach *et al.*, Comp. Phys. Comm. **79** (1994) 503.

[16] D. Karlen, Nucl. Phys. **B289** (1987) 23.

[17] M. Caffo, R. Gatto and E. Remiddi, Phys. Lett. **B173** (1986) 91;
M. Caffo, R. Gatto and E. Remiddi, Nucl. Phys. **B286** (1987) 293.

[18] E. Falk, V. Hedberg and G. von Holtey, CERN SL/97-04(EA).

[19] G. Montagna *et al.*, Nucl. Phys. **B452** (1995) 161;
G. Montagna *et al.*, Nucl. Phys. **B541** (1999) 31.

[20] DELPHI Collaboration, P. Abreu *et al.*, Z. Phys. **C74** (1997) 577.

[21] OPAL Collaboration, R. Akers *et al.*, Z. Phys. **C65** (1995) 47.

[22] D. Dicus and S. Nandi, Phys. Rev. **D56** (1997) 4166;
A. Brignole *et al.*, Nucl. Phys. **B526** (1998) 136.

[23] J.A. Grifols, Pramana **51** (1998) 135.

[24] F. Ferrer and J.A. Grifols, Phys. Rev. **D56** (1997) 7466;
A. Brignole *et al.*, JHEP 9909:002, 1999.

[25] S. Katsanevas and P. Morawitz, Comp. Phys. Comm. **112** (1998) 227.

[26] A.L. Read, DELPHI 97-158 PHYS 737;
     E Gross, A.L. Read and D. Lellouch, Proc. of "12e Rencontres de Physique de la Vallée d'Aoste", M Greco INFN, Frascati, 1998 Frascati physics series 12 (599-628).

[27] J. L. Lopez and D.V. Nanopoulos, Phys. Rev. **D55** (1997) 4450.

[28] The CDF collaboration, F. Abe *et al.*, Phys. Rev. Lett. **81** (1998) 1791.